VII International Conference on Textile Composites and Inflatable Structures
STRUCTURAL MEMBRANES 2015
E. Oñate, K.-U.Bletzinger and B. Kröplin (Eds)

A COUPLED MULTI-SCALE APPROACH FOR THE SIMULATION OF TEXTILE MEMBRANES

B. Kaiser*, E. Haug†, T. Pyttel* and F. Duddeck◇

* Technische Hochschule Mittelhessen - University of Applied Sciences
Wilhelm-Leuschner-Straße 13,61169 Friedberg, Germany
e-mail: benjamin.kaiser@m.thm.de, thomas.pyttel@m.thm.de

† Retired; e-mail: eberhard.haug@esi-group.com, web page: http://www.esi-group.com

◇Technische Universität München
Arcisstr. 21, 80333 München, Germany
e-mail: duddeck@tum.de, web page : http://www.cm.bgu.tum.de

Key words: Draping, Multi-scale, Textile Composites

Abstract. The presented work deals with the simulation of problems related to dry fabric materials. Especially draping over double curved molds is a huge field for industrial simulation methods. Although industrial solutions are available, there are still many open issues. The main reason for these issues is the fact that the mechanical behavior of dry fabric layers is not describable with a standard continuum mechanical approach because the fabric is not a continuum. The idea of the approach presented here is to model the inner structure of the fabric with a unit cell consisting of crossed beams and to couple this inner structure with a macroscopic membrane element (coupled multi-scale approach).

1 INTRODUCTION

In [1] a cross beam model is presented. It is developed for the implicit Software PAM LISA [2]. This cross beam model is embedded in a FE formulation of an elastic Lagrange membrane element [3] in convected coordinates. At each Gauss point a unit cell with crossed beams is implemented instead of a classical constitutive law. Shearing is not considered in that unit cell. Hence shearing effects are taken into account via a elastic membrane material.

This paper proposes a way to implement inner structures in the user material environment of the industrial explicit FE software PAM-Crash[4] by using a similar approach, and is a starting point for more complex extensions for this method. Referring to [1] the implemented inner structure is developed for plain weave fabrics.

2 KINEMATICS

The user material environment for shell elements MAT180 in PAM-Crash is reduced to a membrane by using one Gauss point over thickness. Input variables for the user routine are strain increments, the deformation gradient as well as the node coordinates of the element. With the node coordinates the kinematics can be formulated in convected coordinates independent from the element formulation in PAM-Crash.

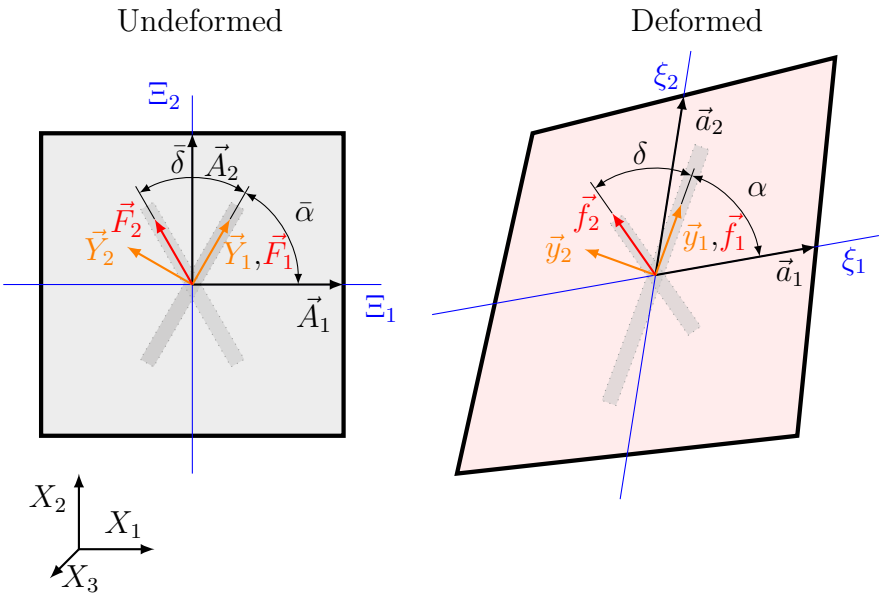

Figure 1: Undeformed and deformed element with coordinate systems

The used coordinate systems are represented by their respective base vectors in Figure 1. To define the kinematics four coordinate systems are needed:

- global Cartesian coordinate system X_i
- local Cartesian coordinate system Y_α,y_α
- local natural convected coordinate system A_α,a_α
- fiber normalized convected coordinate system F_α,f_α

The coordinate lines Ξ_α, ξ_α with the base vectors A_α,a_α are material related. Y_α and y_α are orthogonal Cartesian coordinate systems in the undeformed and deformed membrane element which act in the same plane as Ξ_α and ξ_α rotated around the angle $\bar{\alpha}$ and α. The fiber system directions F_1,f_1 are showing in warp fiber direction, direction F_2,f_2 in weft fiber direction. Angle α is the rotation between the first fiber direction and the first axis of the natural convected coordinate system. Angle δ is the fiber shear angle. The bar symbol over the angle $\bar{\alpha}$ and $\bar{\delta}$marks the reference configuration.

With the convected base in the reference configuration A_α, the metric can be written as,

$$A_{\alpha\beta} = \boldsymbol{A}_\alpha \cdot \boldsymbol{A}_\beta \tag{1}$$

and in the current configuration as

$$a_{\alpha\beta} = \boldsymbol{a}_\alpha \cdot \boldsymbol{a}_\beta \quad . \tag{2}$$

The components of the Green-Lagrange strain tensor $\alpha_{\alpha\beta}$ in the $\boldsymbol{A}_\alpha$ base can be written as,

$$\alpha_{\alpha\beta} = \frac{1}{2}(a_{\alpha\beta} - A_{\alpha\beta}) \quad . \tag{3}$$

With the transformation rule [3],

$$Y_\alpha = \bar{d}_\alpha^\beta \cdot A_\beta \tag{4}$$

where $\bar{d}_\alpha^\beta$ is

$$\begin{pmatrix} \bar{d}_1^1 & \bar{d}_1^2 \\ \bar{d}_2^1 & \bar{d}_2^2 \end{pmatrix} = \begin{pmatrix} \frac{1}{\sqrt{A_{11}}}\cos\bar{\alpha} - \frac{A_{12}}{\sqrt{A \cdot A_{11}}}\sin\bar{\alpha} & \sqrt{\frac{A_{11}}{A}}\sin\bar{\alpha} \\ -\frac{1}{\sqrt{A_{11}}}\sin\bar{\alpha} - \frac{A_{12}}{\sqrt{A \cdot A_{11}}}\cos\bar{\alpha} & \sqrt{\frac{A_{11}}{A}}\cos\bar{\alpha} \end{pmatrix} \tag{5}$$

the coordinates of the Green-Lagrange strain tensor can be transformed in the Cartesian system Y_α by

$$E_{\alpha\beta} = \bar{d}_\alpha^\gamma \bar{d}_\beta^\delta \alpha_{\gamma\delta} \ , \ \boldsymbol{E} = E_{\alpha\beta}\vec{Y}_\alpha \otimes \vec{Y}_\beta \quad . \tag{6}$$

From the transformation A_{12} and A_{11} are components of $A_{\alpha\beta}$ and A is

$$A = \det(A_{\alpha\beta}) \quad . \tag{7}$$

To get the strain of the fibers it is nessesary to transform the strain $E_{\alpha\beta}$ in the fiber system. The transformation for the base vectors Y_β to the fiber system F_α is

$$F_\alpha = \bar{c}_\alpha^\beta \cdot Y_\beta, \tag{8}$$

where $\bar{c}_\alpha^\beta$ is

$$\begin{pmatrix} \bar{c}_1^1 & \bar{c}_1^2 \\ \bar{c}_2^1 & \bar{c}_2^2 \end{pmatrix} = \begin{pmatrix} 1 & 0 \\ \cos\bar{\delta} & \sin\bar{\delta} \end{pmatrix} \quad . \tag{9}$$

The Green-Lagrange strain in the fiber system follows as

$$\beta_{\alpha\beta} = \bar{c}_\alpha^\gamma \bar{c}_\beta^\delta E_{\gamma\delta} \quad . \tag{10}$$

With the general definition of the Green-Lagrange strain [5]

$$d\boldsymbol{x} \cdot d\boldsymbol{x} - d\boldsymbol{X} \cdot d\boldsymbol{X} = l^2 - L^2 = 2d\boldsymbol{X} \cdot \boldsymbol{E} d\boldsymbol{X} \quad , \tag{11}$$

the strain in fiber direction 1 can be written as

$$\beta_{11} = \frac{1}{2}\frac{l_1^2 - L_1^2}{L_1^2}. \tag{12}$$

With the known warp fiber length L in the reference configuration, the actual fiber length l can be calculated based on formula (12) by

$$l_1 = \sqrt{2 \cdot \beta_{11} + 1} \cdot L_1 \quad . \tag{13}$$

The displacement of a unit cell in fiber direction 1 follows as

$$u_1 = l_1 - L_1 = \sqrt{2 \cdot \beta_{11} + 1} \cdot L_1 - L_1. \tag{14}$$

The same is applied to fiber direction 2. These displacements can be seen as movements of master-nodes with regard to a homogenization method. In [6] and [7] a master node concept is shown to calculate linear elastic material properties. This could be used to implement general unit cells.

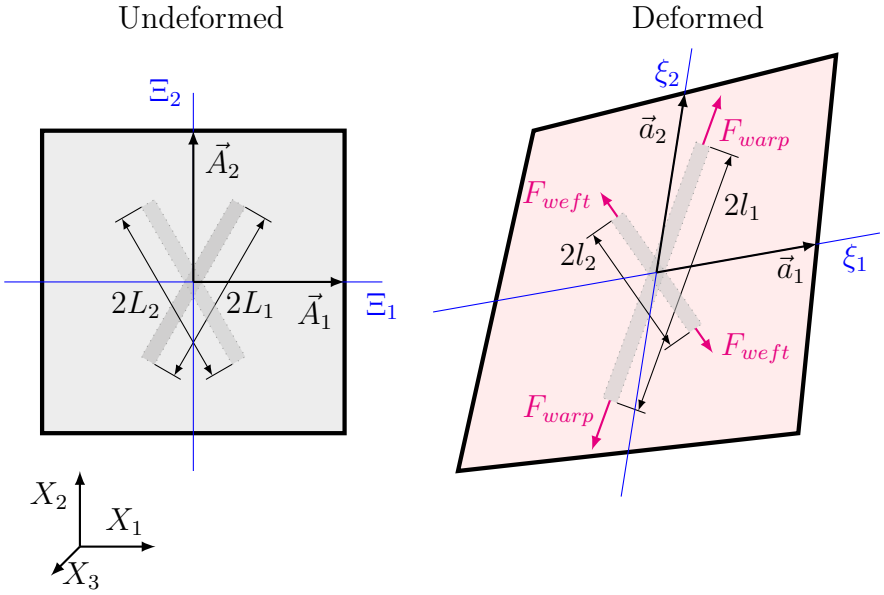

Figure 2: Undeformed and deformed element with fibers

3 KINETICS

From a given force F_{warp} and F_{weft} in fiber directions, shown in picture 2, the stress in the element can be calculated. The PAM-Crash user material uses Cauchy stresses as stress quantity. With the fiber length, L_2, and standard thickness $t = 1$ the one dimensional first Piola-Kirchhoff (1st PK) stress in fiber direction are calculated as

$$P_{11} = \frac{F_{warp}}{L_2 \cdot t} \ , \ P_{22} = \frac{F_{weft}}{L_1 \cdot t} \quad . \tag{15}$$

In order to get the second Piola-Kirchhoff (2nd PK) stress the transformation [8]

$$\boldsymbol{S} = \boldsymbol{F}^{-1} \cdot \boldsymbol{P} \tag{16}$$

is used. The 2nd PK is formulated in the reference configuration. The deformation gradient $\boldsymbol{F}$ for the 1D case in fiber direction is given as

$$F_{11} = \lambda_1 = \frac{l_1}{L_1}. \tag{17}$$

So the 2nd PK stress components m_{11} for warp Fiber in the fiber system F_α can be written as

$$m_{11} = F_{11}^{-1} \cdot P_{11} = \frac{P_{11}}{\lambda_1} \tag{18}$$

The component m_{12} and m_{21} are zero so the components of $m_{\gamma\delta}$ can be written as

$$m_{\alpha\beta} = \begin{pmatrix} m_{11} & 0 \\ 0 & m_{22} \end{pmatrix} \quad . \tag{19}$$

In order to get the 2nd PK stress in the Cartesian system Y_α, $m_{\gamma\delta}$ is transformed by using(8)

$$S_{\alpha\beta} = \bar{c}^{\alpha}_{\gamma}\bar{c}^{\beta}_{\delta} m_{\gamma\delta} \ , \ \boldsymbol{S} = S_{\alpha\beta}\vec{Y}_\alpha \otimes \vec{Y}_\beta \quad . \tag{20}$$

With

$$\boldsymbol{\sigma}_{cross\ beam} = J^{-1} \cdot \boldsymbol{F} \cdot \boldsymbol{S} \cdot \boldsymbol{F}^T, \tag{21}$$

the 2nd PK stress can be transformed to Cauchy stresses, where $\boldsymbol{\sigma}_{cross\ beam}$ is the stress part coming from the cross beam model. In (21), $\boldsymbol{F}$ is the deformations gradient in the membrane element which is defined as

$$\boldsymbol{g}_\alpha = \boldsymbol{F}\boldsymbol{G}_\alpha \quad , \tag{22}$$

and J is the Jacobian determinate

$$J = \det(\boldsymbol{F}). \tag{23}$$

The computed stresses in the membrane element are equivalent to the forces in the unit cell.

4 MATERIAL LAW

4.1 Cross beam model

Picture 3 shows a deformed membrane element with inner structure. Warp and weft fiber directions are pointing in the direction of the convected base vectors. That means the value of angle $\bar{\alpha}$ is 0°. Because of visibility this example has only one unit cell, which is equivalent to an under-integrated element with one Gauss point. Fully integrated elements are possible in the same way. In red the warp and in green the weft fiber is pictured. The contact element is shown in light blue.

In the kinematics section a way is shown to solve displacements for a fiber. With these displacements a unit cell is loaded on the master nodes N_1 and N_2 shown in figure 4. The material model, shown in this section, is based on a unit cell for a plain weave fabric. The unit cell is modeled with three beam elements. Because of symmetry only half of the unit cell is modeled. In Figure 4 the 3D unit cell is shown in 2D where $\vec{f}_1$ and $\vec{f}_2$ are falling together. The warp fiber is modeled with beam element 1, the weft fiber is modeled with

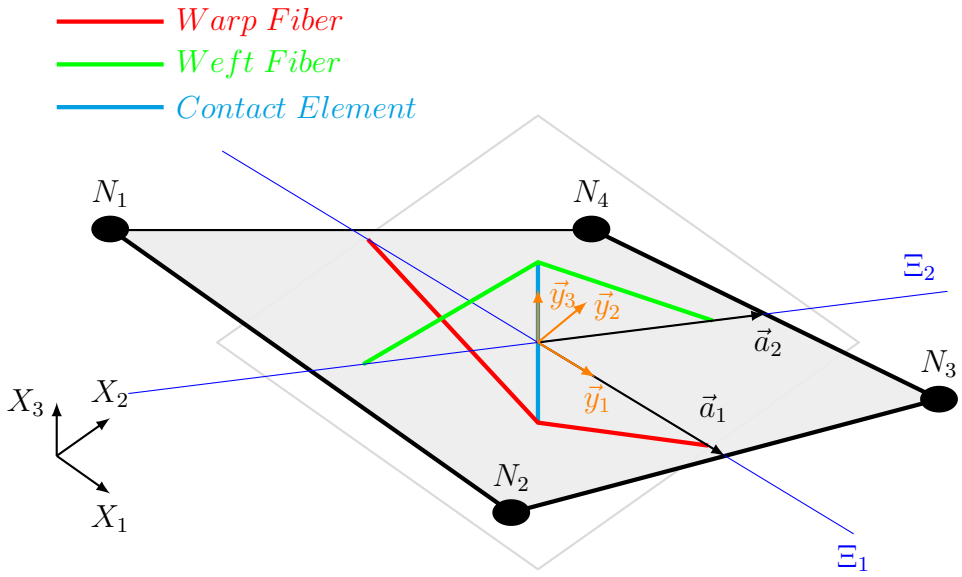

Figure 3: Membrane element with inner structure

beam element 2 and the contact between the fibers is represented by beam 3.

For the shown discrete mechanical system, the global stiffness matrix K can be constructed with K_E the elastic and K_G the geometrical stiffness matrix.

$$K = K_E + K_G \tag{24}$$

The global stiffness matrix K_E consists of the Young's moduli of the fibers, which are E_{warp} and E_{weft}, the contact Young's modulus E_3, as well as the geometrical properties of the fiber I_{warp}, I_{weft}, which are the second moment of inertia of the beams, the cross-sections of the fibers A_{warp}, A_{weft} and the dimensions L_1, L_2, L_3.

The system of equations can be then written as follows.

$$\begin{pmatrix} F_{warp} \\ F_{weft} \\ 0 \\ 0 \end{pmatrix} = \begin{pmatrix} K_{11} & K_{12} & K_{13} & K_{14} \\ K_{21} & K_{22} & K_{23} & K_{24} \\ K_{31} & K_{32} & K_{33} & K_{34} \\ K_{41} & K_{42} & K_{43} & K_{44} \end{pmatrix} \cdot \begin{pmatrix} u_1 \\ u_2 \\ u_3 \\ u_4 \end{pmatrix} \quad . \tag{25}$$

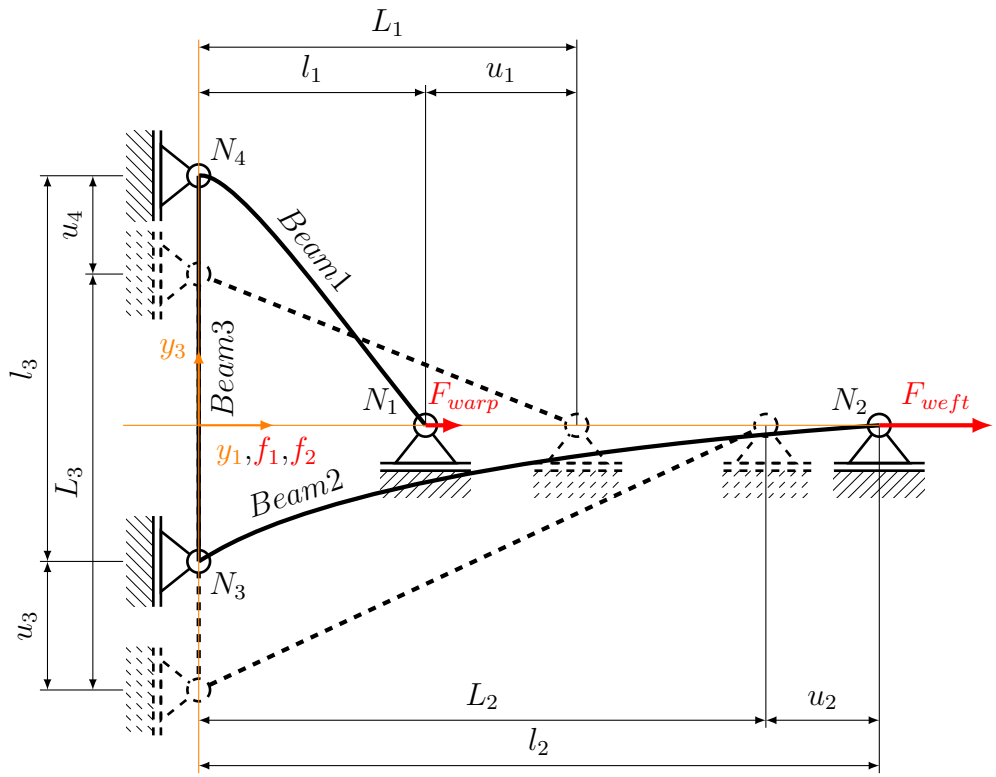

Figure 4: Discrete mechanical system

Due to the dependency of K_G on the force F_{warp} and F_{weft}, the system of equations is nonlinear and has to be solved iteratively. With the so computed forces, stresses can be calculated like shown in section kinetics.

4.2 Shear

Shear is modeled by a second layer of a material with a linear elastic shear behavior. The material law is defined in the reference configuration. Due to the symmetry of the 2nd PK stress S_{ij}, the constant model for this layer can be written as

$$\begin{pmatrix} S_{11} \\ S_{22} \\ S_{12} \end{pmatrix} = \begin{pmatrix} 0 & 0 & 0 \\ 0 & 0 & 0 \\ 0 & 0 & G_{12} \end{pmatrix} \cdot \begin{pmatrix} E_{11} \\ E_{22} \\ E_{12} \end{pmatrix} \quad , \tag{26}$$

where G_{12} is the constant shear modulus and E_{ij} the components of the Green-Lagrange strain tensor. With (21) the 2nd PK stress $\boldsymbol{S}$ is transformed to Cauchy stress $\boldsymbol{\sigma}_{shear}$. The total Cauchy stress in the membrane element is the sum of the shear stress and the stress coming from the cross beam model. The returned stress to PAM-Crash is

$$\boldsymbol{\sigma} = \boldsymbol{\sigma}_{shear} + \boldsymbol{\sigma}_{cross\ beam} \quad . \tag{27}$$

5 RESULTS

As test case for the validation of the cross beam model, a double dome test is chosen. The tool FE mesh is taken from a double-dome benchmark which has been performed by several labs shown at `http://www.wovencomposites.org` in order to validate and compare different approaches. Figure 5 shows the FE geometry of the draping test with fabric (red), blank holder (green), die (dark grey) and punch (light grey). In the publications [9] and [10], a draping experiment was done with the same tools geometry. Experimental results are taken from these publications. The used plain weave fabric in the experiment

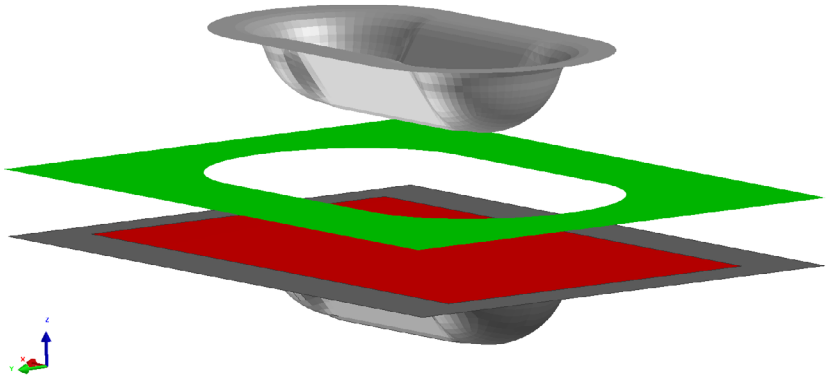

Figure 5: Double dome benchmark model

was a Twintex TPEET22XXX. The material properties of that fabric were studied in the publications [11] and [12]. The roving of the fabric is a $12k$ roving. The specimen size is 470 mm x 270 mm. In the simulation only a quarter is simulated because of symmetry reasons. The used material properties can be found in Table 1. The Young's modulus

Table 1: Material parameters

E_{weft},E_{warp}	35.4	kN/mm^2
E_3	1	kN/mm^2
shear modulus G_{12}	0.001	kN/mm^2
Cross-section A_{weft},A_2	1.0	mm^2
Cross-section A_{warp}	17.6	mm^2
second moment of inertia I_1,I_2	$1.0e^{-4}$	mm^4
L_1,L_2	2.5	mm
L_3	0.8	mm

E_3 for the contact beam element is an assumption. The cross-section for beam 3 is the contact area of two rovings in the plain weave fabric.

The simulation results from the cross beam model of the double dome test are shown in Figure 6. On the left side the draw-in of the fabric is compared with the draw-in of the double dome experiment from [9]. The green line is extracted from the experiment picture in that publication. The draw-in can be simulated well with the cross beam model. Only small differences at the corners can be found which are in the measuring accuracy. At the right side of Figure 6 the fiber direction and the points for the shear

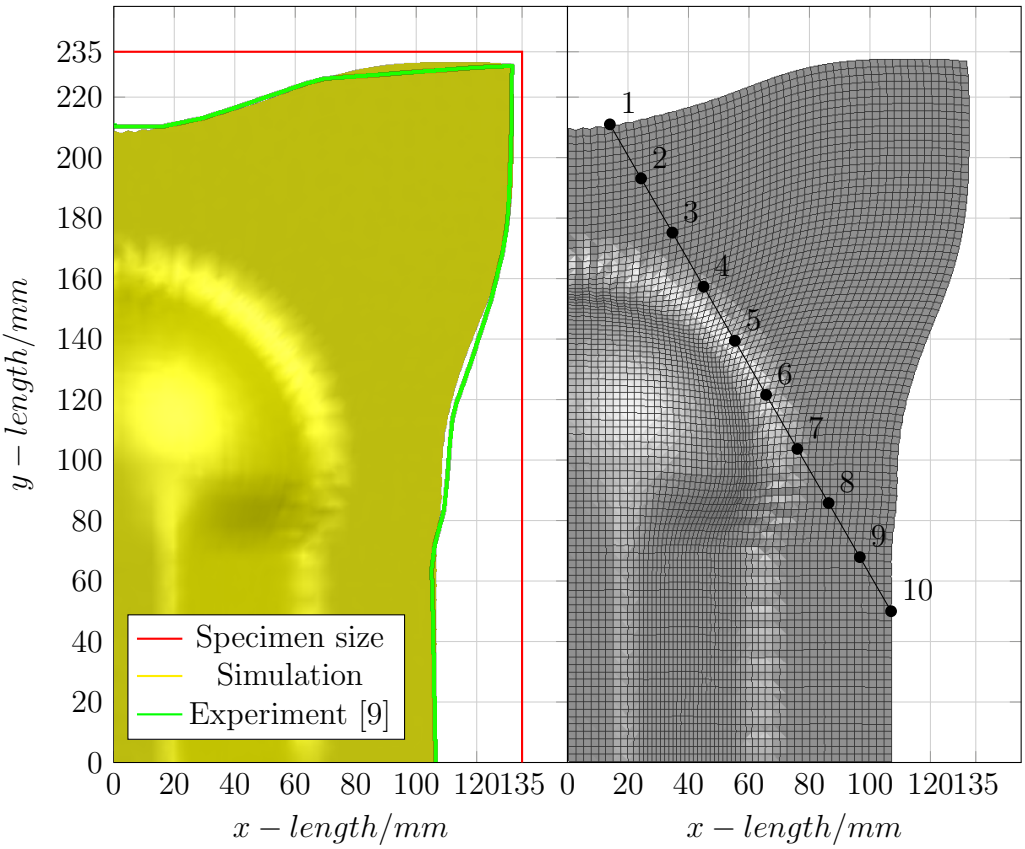

Figure 6: Double dome test - experiment vs. simulation

angle measurements are shown. The points from 1 to 10 are on a diagonal line from the corner points of the undeformed specimen $(0, 235)$ and $(135, 0)$. Point 1 and 10 are on the border of the deformed part. The line segment from point 1 to 10 is divided in 9 even parts to build point 2 to 9. The shear angle of the experiment and the simulation is compared in Diagram 7. The characteristics of the curves from experiment and simulation

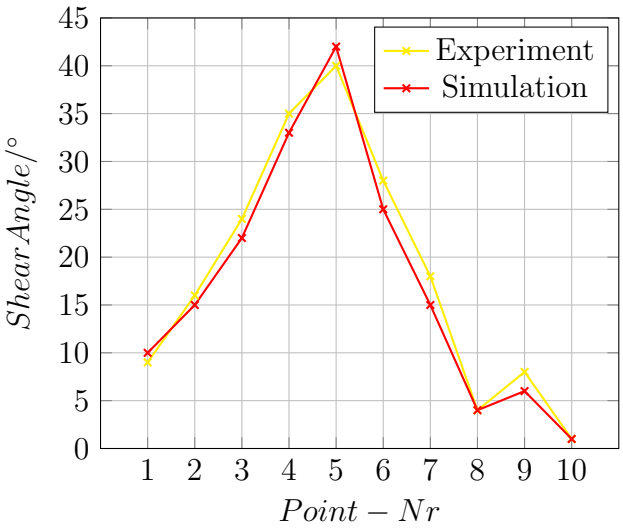

Figure 7: Shear angle - experiment vs. simulation

are comparable , with one high peak at point 5 in the area of the major shear deformation and a small peak at point 9 where shearing is getting larger because of the hemisphere geometry of the double dome.

6 CONCLUSIONS

Draping problems can be solved with a coupled multi-scale approach. For the implemented inner structure for plain weave fabrics the approach delivers good results. Draw-in of the fabric sheet while draping can be reproduced. Also the shearing between the fibers can be predicted.

In a next step, the coupling between the inner structure and the membrane element will be generalized for periodic fabric materials, to couple an arbitrary representative volume element at Gauss point level. Also an extension to describe bending is planned.The presented work is related to draping, but the method offers new opportunities for any application where the inner structure of a material plays an important role.

REFERENCES

[1] E. Haug, P. De Kermel, B. Gawenat, and A. Michalski. Industrial design and analysis of structural membranes. In *International Conference on Textile Composites and Inflatable Structures STRUCTURAL MEMBRANES*, Barcelona, Spain, 2007.

[2] ESI Group, 100-102 Avenue de Suffren 75015 Paris. *PAM-LISA Manual Volume 1 - Theory.*

[3] E. Haug and G.H. Powell. Finite element analysis of nonlinear membrane structures. Technical Report UC SESM 72-7, Structural Engineering Laboratory, University of California, Berkeley, USA, February 1972.

[4] ESI Group, 100-102 Avenue de Suffren 75015 Paris FR. *PAM-Crash Solver Reference Manual*, 2013 edition.

[5] H. Parisch. *Festkörper-Kontinuumsmechanik.* Vieweg Teubner, 2003.

[6] B. Kaiser. Wickelsimulation und Homogenisierung von glasfaserverstärkten Kunststoffrohren. Master's thesis, Fachhochschule Gießen-Friedberg, Germany, 2010.

[7] D. Lukkassen, L.-E. Persson, and P. Wall. Some engineering and mathematical aspects on homogenization method. *Composites Engineering*, 5(5):519–531, 1995.

[8] T. Belytschko, W. K. Liu, B. Moran, and K. I. Elkhodary. *Nonlinear Finite Elements for Continua and Structures.* Wiley, 2014.

[9] M.A. Khan, T. Mabrouki, E. Vidal-Sall, and P. Boisse. Numerical and experimental analyses of woven composite reinforcement forming using a hypoelastic behaviour. Application to the double dome benchmark. *Journal of Materials Processing Technology*, 210(2):378 – 388, 2010.

[10] S. Gatouillat, A. Bareggi, E. Vidal-Salle, and P. Boisse. Meso modelling for composite preform shaping - simulation of the loss of cohesion of the woven fibre network. *Composites Part A: Applied Science and Manufacturing*, 54:135–144, 2013.

[11] J. Cao, R. Akkerman, P. Boisse, J. Chen, H.S. Cheng, E.F. de Graaf, J.L. Gorczyca, P. Harrison, G. Hivet, J. Launay, W. Lee, L. Liu, S.V. Lomov, A. Long, E. de Luycker, F. Morestin, J. Padvoiskis, X.Q. Peng, J. Sherwood, Tz. Stoilova, X.M. Tao, I. Verpoest, A. Willems, J. Wiggers, T.X. Yu, and B. Zhu. Characterization of mechanical behavior of woven fabrics: Experimental methods and benchmark results. *Composites Part A: Applied Science and Manufacturing*, 39(6):1037–1053, 2008.

[12] J. Launay, G. Hivet, A. V. Duong, and P. Boisse. Experimental analysis of the influence of tensions on in-plane shear behaviour of woven composite reinforcements. *Composites Science and Technology*, 68(2):506 – 515, 2008.